BUCKLE PROPAGATION OF SANDWICH PIPES UNDER EXTERNAL PRESSURE

(DOI No: 10.3940/rina.ijme.2020.a1.536a)

C An, College of Safety and Ocean Engineering, China University of Petroleum (Beijing), Beijing, China; **B Q Liu,** Ocean Engineering Program, Federal University of Rio de Janeiro, Rio de Janeiro, Brazil; **T T Li**, College of Safety and Ocean Engineering, China University of Petroleum (Beijing), China; **G M Fu**, School of Petroleum Engineering, China University of Petroleum (East China), Qingdao, China; **M L Duan**, College of Safety and Ocean Engineering, China University of Petroleum (Beijing), Beijing, China.

SUMMARY

Buckle propagation of local collapse appearing in the damaged pipes is one of the failure modes that are of particular interest for deepwater application. The local collapse can propagate along the pipeline for long distances in both directions when the external pressure magnitude is up to the propagation pressure. In this paper, the buckle propagation pressure of sandwich pipes (SP) with different material properties and geometric characteristics is investigated by numerical simulation using Python programming language based on general finite element code. The results of the pressure history data obtained are verified by comparing those published previously. The effect of material properties, geometric characteristics and adhesion conditions on the propagation pressure are analyzed.

1. INTRODUCTION

With the global marine resources being developed in full swing, the focus of offshore oil and gas exploration and development has shifted from shallow water to deep water. Since the failure of deepwater pipeline may lead to enormous economic cost and even environmental disaster, research on pipeline behavior under typical loads, such as external hydrostatic pressure, is very important for oil/gas transportation.

Buckle propagation phenomenon starts from a locally weakened section of the pipe, such as a dent induced by impact by a foreign object, a local buckle resulting from excessive bending during installation or a wall thickness reduction caused by wear or corrosion (Kyriakides and Corona, 2006). During the buckle propagation along the pipelines, the pipe inner walls come into contact. As a result, the transportation capacity of the pipeline will degrade. Buckle and collapse due to external pressure play an important role in the design of such tubular structures. The minimum pressure required for buckling propagation is the propagation pressure (Pp). One of the earliest attempts to determine the propagation pressure analytically was presented by Palmer and Martin (1975). Kyriakides and Bobcock (1981) carried out extensive theoretical and experimental study on buckle propagation and arrest phenomena of externally pressurized pipes. After that, many experimental and numerical studies were conducted to investigate the buckle propagation pressures for different material characteristics and geometric parameters (Showkati and Shahandeh, 2010; Albermani *et al*., 2011; Gong *et al*., 2012; Khalilpasha and Albermani, 2014). The propagation pressure primarily depends on geometric characteristics and material properties of the pipes (Dyau and Kyriakides, 1993), which is usually 15-30% of the collapse pressure of intact pipes (Gong *et al*., 2013). Besides, buckle propagation of pipe-in-pipe systems were studied through extensive experimental studies and numerical simulations (Kyriakides, 2002; Kyriakides and Vogler, 2002; Kyriakides and Netto, 2004).

To achieve flow assurance in extreme deep water environment, sandwich pipes (SP), combining high structural resistance with thermal insulation capability, have attracted considerable research interest over the last few years. Sandwich pipe consists of two concentric metal pipes in which the annulus is filled with a proper material that combines structural strength and thermal insulation in an optimized design (Estefen *et al*. 2005). An analytical approach using energy method was proposed by Arjomandi and Taheri (2010) for estimating the bucking capacity of sandwich pipes. The interfacial adhesion characteristics between annular core and pipes affect much the structural integrity of SP. Castello and Estefen (2007) studied the effect of interfacial adhesion degree between polypropylene core and API X-60 tubes on the collapse pressure of SP. Based on the results of 2400 finite element models developed using the parametric modeling procedure, He *et al*. (2015) proposed a simplified practical equations to calculate the pressure capacity of sandwich pipes with different inter-layer bonded strengths. Xu *et al*. (2016) conducted shear tests of SP section to determine the interface adhesion between the polypropylene core layer and surrounding steel pipes. Besides polymer, high performance cement-based material can be another choice for the annular core, based on the characteristics of high fracture toughness and good adhesion with metal. An *et al*. (2012) investigate the collapse behavior of SP with steel fiber reinforced concrete under external pressure using finite element method. An *et al*. (2014) reported the experimental results of the hyperbaric chamber collapse tests for the full-scale SP filled with PVA fiber reinforced cementitious composites. Fu *et al*. (2014) investigated numerically the buckle propagation of SP by using the commercial finite element package.

Although some experimental and numerical results of buckle propagation of SP under external pressure were

summarized by An *et al*. (2013), the influence of material characteristics, geometric parameters and adhesive properties on the buckle propagation behavior needs to be further estimated. In this paper, a three-dimensional finite element model of buckle propagation for SP is developed and verified by comparing the numerical results with the one published previously. Using Python script language, 96 SP models with various parameters are generated, which are employed to analyze the influence of material characteristics, geometric parameters and adhesive properties on the buckle propagation pressure of SP.

2. FINITE ELEMENT MODELLING

The massive simulation of the buckle propagation phenomenon of different sandwich pipes in the pressure chamber are realized by the parametric modeling method. As shown in Figure 1, the general routine of this method is firstly generating the ABAQUS input files for the buckle propagation pressure of sandwich pipes in the hyperbaric chamber for parametric study based on a Python program. Secondly, the model generated by the Python code is transferred into the ABAQUS kernel to simulate the buckle propagation progress through ABAQUS scripting interface. After simulation, the buckle propagation pressure is extracted and processed from the output database (ODB) files. The parametric modeling method can greatly simplify the simulation process and improve the computational efficiency.

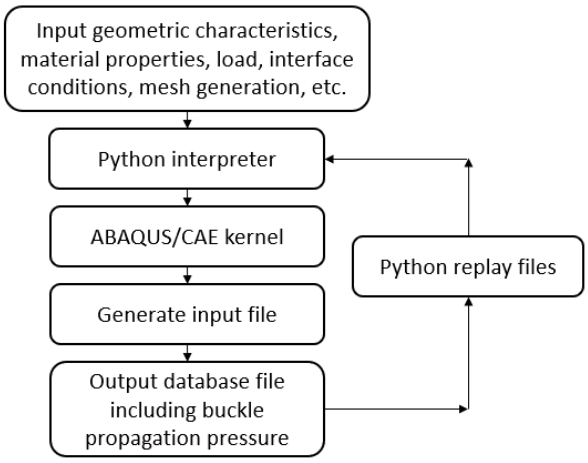

Figure 1: Flowchart of the parametric modeling method

For the quasi-static buckle propagation analysis of SP under external pressure, the Newton-Raphson iteration methods are not suitable for buckle problems and often fail in the neighborhood of critical points. To overcome this problem and trace the equilibrium paths through limit points into the post-critical range, the Arc-length type method is employed in the present study. Automatic increment control scheme with variable loading increments is adopted.

2.1 MATERIAL CHARACTERISTICS

For deep-water pipelines, carbon manganese steel is generally used as the pipe material, which has a significant yield point and plastic deformation capacity. Ramberg-Osgood (R-O) model described by Eq. (1) is used to describe the constitutive relation of steel:

$$\varepsilon = \frac{\sigma}{E}\left[1+\frac{3}{7}\left|\frac{\sigma}{\sigma_y}\right|^{n-1}\right] \tag{1}$$

where E is the elastic modulus, σ stress, ε strain, σ_y the yield stress and n the material hardening parameter. The R-O constitutive model can better fit the stress-strain relationship of steel when the strain is small, but the gradually increasing deviation appears as the strain becomes large. The buckle propagation problem is a phenomenon happened after the local collapse of the pipes, which belongs to the post-buckling phenomenon with the large strain stage. To predict the behavior of the post-buckling, it is required that the accurate plastic information of materials including the large strain stage should be given, which the normal R-O model cannot achieve. To compensate the drawback of R-O model, a modified R-O model described by Eq. (2) is used to fit the stress-strain curve of steel, where the curve for strain larger than 0.015 is approximated using a straight line, as suggested by Gong *et al*. (2012) and Gong *et al*. (2013).

$$\varepsilon = \begin{cases} \dfrac{\sigma}{E}\left[1+\dfrac{3}{7}\left|\dfrac{\sigma}{\sigma_y}\right|^{n-1}\right], & \varepsilon<0.015 \\ \dfrac{1}{E'}(\sigma-\sigma_{1.5})+0.015, & \varepsilon\geq 0.015 \end{cases} \tag{2}$$

where E' is defined by

$$E' = \left.\frac{d\sigma}{d\varepsilon}\right|_{\varepsilon=0.015} = \frac{E}{1+\dfrac{3}{7}n\left|\dfrac{\sigma}{\sigma_y}\right|^{n-1}} \tag{3}$$

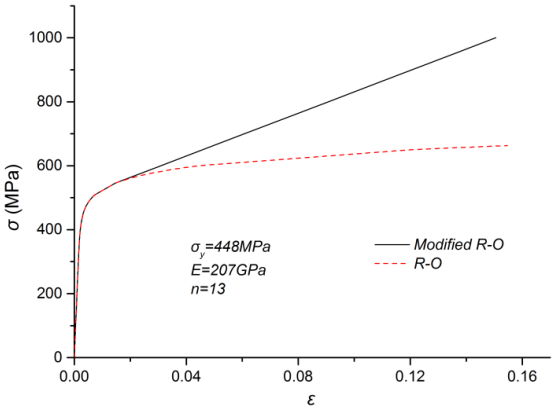

Figure 2: Modified Ramberg-Osgood stress-strain curve for X65

Figure 2 shows the modified stress-strain curve for X65 steel grade fitted by R-O and modified R-O models, where the yield stress σ_y and the corresponding strain are 448 MPa and 0.005, respectively, according to API 5L. The material characteristics of polypropylene for the annular layer refers to Estefen *et al*. (2005), as shown in Figure 3.

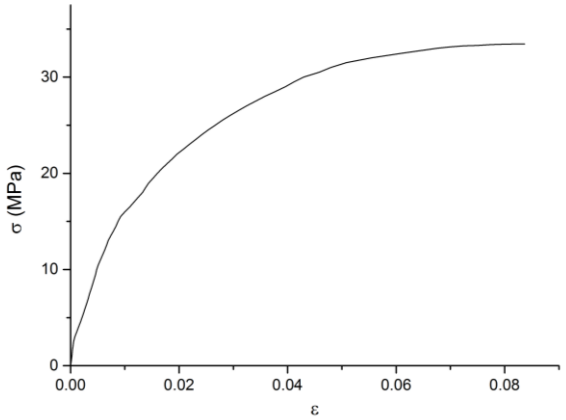

Figure 3: Tensile stress-strain curve of Polypropylene

2.2 ELEMENT TYPE AND MESH GENERATION

C3D27, a three-dimensional quadratic brick elements with twenty-seven nodes, provided by ABAQUS is chosen to model the inner and outer tubes. This type of element has an accurate solution of displacement and stress, which can overcome shear locking phenomenon for the subsequent contact problems during the buckle propagation process. Besides, C3D27H, a three-dimensional, twenty-seven nodes, quadratic hybrid elements, is employed to model the annular layer. The mesh-sensitivity analysis is carried out to consider the effect of element sizes on the convergence of propagation pressure. Each steel pipe is discretized into 14 elements around the quarter circumference, 40 elements along the length, while the annular layer is discretized into 3 elements through the thickness. In addition, the element mesh is refined near $\theta = 0°$ and $\theta = 90°$ as shown in Figure 4.

The contact is simulated by using the surface-based contact model, which prevents the nodes on the inner surface of the SP from penetrating the planes of symmetry. A volume-controlled loading procedure is adopted using the hydrostatic fluid element F3D4, which can indicate the volume change inside a control region defined around the SP.

2.3 INTERFACE AND BOUNDARY CONDITIONS

A small-sliding surface-based formulation is used for the contact between the inner surface of the internal pipe and the rigid plane. The contact relationships between pipes and annular layer are assumed to be unbonded and fully-bonded which stands for no adhesion and perfect adhesion, respectively. For the unbonded model, nodes for pipes and annular layer at the interface are generated independently. For fully-bonded case, pipes and annular layer share common nodes at the interface. The tangential behavior between master and slave surfaces is assumed to be frictionless or perfect adhesion. The collapsing layers do not allow separation after contact.

The symmetrical boundary conditions are applied at planes X-Y and X-Z, and the Y-direction and Z-direction displacements of the nodes are fixed but free to expand in the X-direction at X=L.

2.4 GEOMETRY OF INITIAL IMPERFECTIONS

The geometric properties of SP are shown in Table 1 and Figure 5. The values are extracted from the API 5L, where D_n is the nominal diameter, R_i the radius of internal surface, R_e the radius of external surface, L the length, t_1, t_c and t_2 the thickness of inner pipe, annulus and outer pipe, respectively. The cross section of SP is assumed to be circular along the length except that a local imperfection is added near one end of the SP at $x \in (0,0.5D)$, which is the way to initiating local collapse and subsequent buckle propagation. The local imperfection of the three layers are assumed to be identical and defined by Eq. (4).

$$w_0(\theta) = -\Delta_0 \left(\frac{D}{2}\right) exp\left[-\beta \left(\frac{x}{D}\right)^2\right] cos\, 2\theta, \quad x \in (0,0.5D) \tag{4}$$

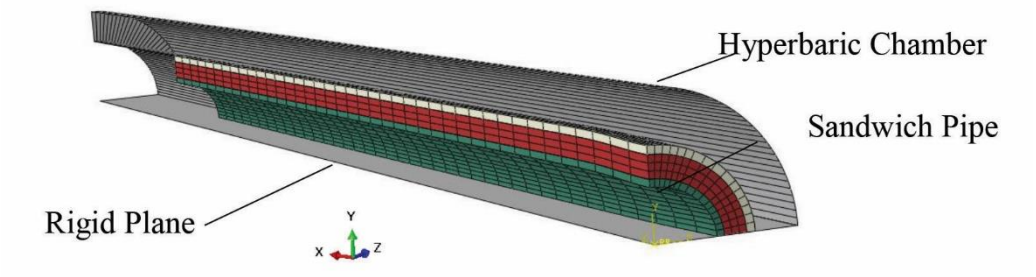

Figure 4: Finite element mesh of the SP

Table 1: Geometric parameters of the SP

	D_n (in)	R_i (mm)	R_e (mm)	t (mm)	L (mm)
Internal pipe	14	168.91	177.80	8.89	5000
Annular layer		177.80	217.17	39.37	5000
External pipe	18	217.17	228.6	11.43	5000

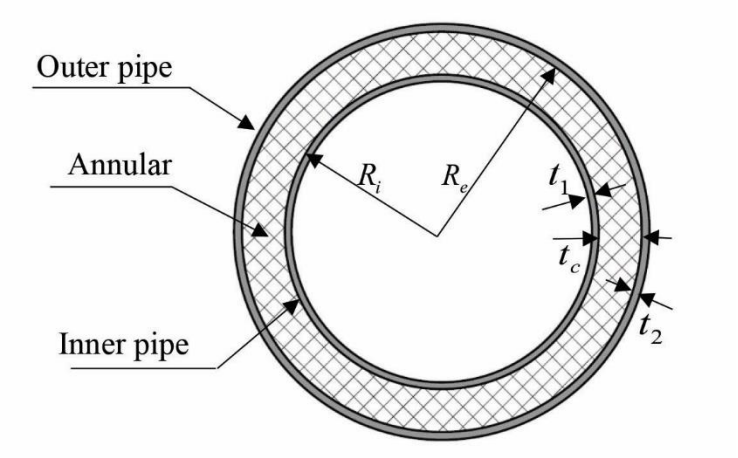

Figure 5: Geometries of the SP

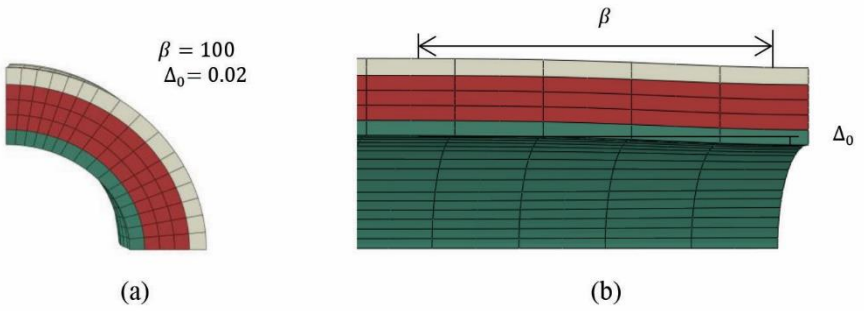

Figure 6: Initial imperfection applied for the SP

where $W_0(\theta)$ is the radial displacement, D the tube diameter, θ the polar angular coordinate, x the axial coordinate, Δ_0 the imperfection amplitude, β the extent of the imperfection. The applied imperfection pattern of SP is shown in Figure 6. The calculated buckle propagation pressure using the imperfection suggested is the conservative assumption, which is the maximum value among the buckle propagation pressure of the SP with various imperfection combination of the inner and outer pipes.

2.5 NUMERICAL SIMULATION RESULTS

Figure 7 shows the calculated pressure-change in volume responses for SP, where V_0 is the initial internal volume of the SP, and ΔV the absolute value of volume change evaluated for each deformed configuration. A sequence of deformed configurations of the SP is also demonstrated in the figure. The initial state of the SP is identified by the Roman number I, after that the pressure monotonically increases. The configuration II shows that the buckle collapse occurs to the SP, which is followed by a sharp decrease in pressure. The configuration III represents the SP with local collapse at the imperfection region. As the opposite walls of the internal pipe meets in the configuration IV, the pressure ceases to drop. The collapse is arrested locally, and the buckle starts to propagate along the downstream direction of the SP. The subsequent pressure plateau represents steady-state propagation of the buckle, and the configuration V shows the profile of buckle propagation of the SP with longer contact length. Eventually, as the buckle propagation terminated at the end of the pipe, which is flattened in the configuration VI.

2.6 VERIFICATION OF MODEL

The proposed finite element model is verified by comparing its results with the ones obtained by Lourenço *et al*. (2008). The geometric parameters of the SP are shown in Table 2. D_i is the internal diameter of the inner pipe. The imperfection amplitude Δ_0 is 0.02, and the extent β is 1. Based on the uniaxial tensile stress-strain curves determined by Netto *et al*. (2002), the hyperelastic Marlow model in ABAQUS is used to describe the material behavior of polypropylene.

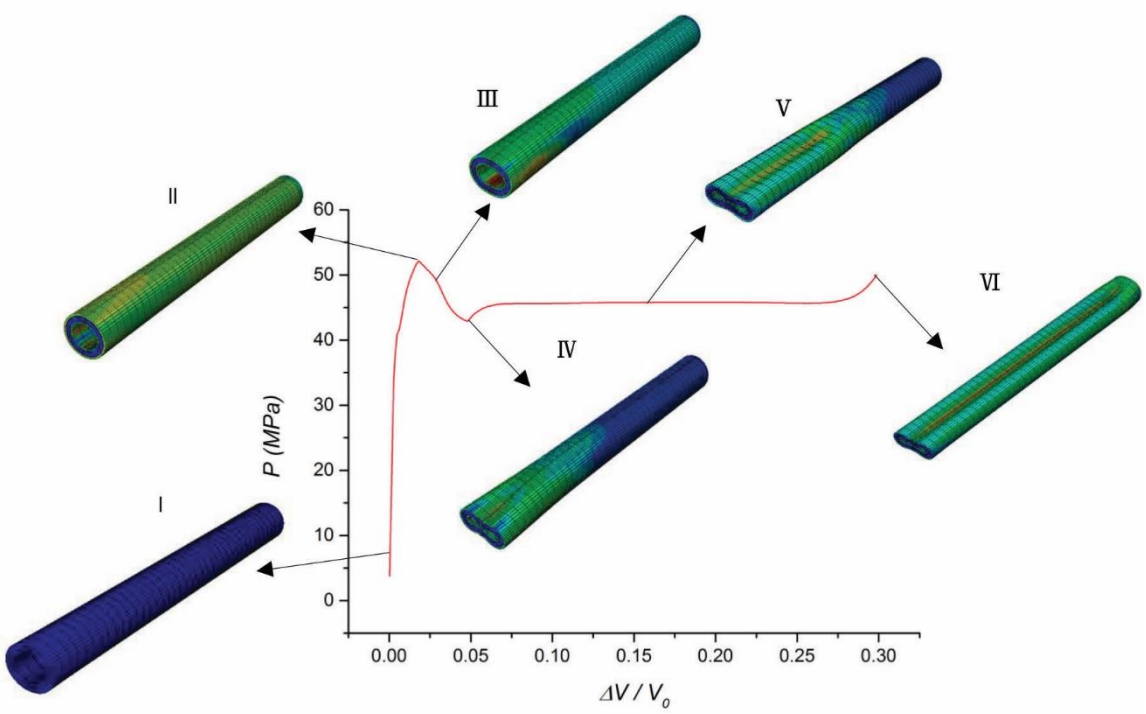

Figure 7: Pressure change in volume response for the SP

Table 2: Geometric parameters of the SP

Model	D_i (mm)	t_1 (mm)	t_c (mm)	t_2 (mm)
SP.G1.P01*	45.83	1.60	11.50	1.64
SP.G1.P02*	46.27	1.71	11.15	1.64
SP.G2.P01*	46.43	1.69	4.82	1.48
SP.G2.P02*	47.06	1.67	4.41	1.49

*: Label of SP employed in Lourenço *et al*. (2008), where G1 and G2 represent two nominal geometric configurations.

As shown in Figure 8, the pressure changes in volume response curves of SP with G2 geometry calculated using the current model is compared with the ones presented by Lourenço *et al*. (2008). It can be seen that the two set of curves have the identical pressure changing trend and the similar pressure values. Results of the buckle propagation pressure are listed in Table 3. The maximum error in Table 3 refers to the comparison between the values obtained in this paper and the ones calculated by Lourenço *et al*. (2008). For instants, the errors of SP.G1.P02 are 0.87% for no adhesion condition and 1.04% for perfect adhesion condition, then the maximum error is 1.04%. Results from the experiments are listed here to indicate the reasonableness of the present method. The maximum difference appears for the no adhesion case of SP.G2.P01, which is 2.68%. The sources of errors are mainly attributed to the difference in the mesh resolution of the model along the radial, circumferential and longitudinal directions.

3. PARAMETRIC STUDY

3.1 INFLUENCE FACTORS OF P_P

The pressure capacity of SP is dependent on the material properties, the geometric characteristics and the relationship between layers, which can be represented as Eq. (5).

$$P_p = F(t_1, r_1, t_2, r_2, \nu_p, \nu_c, E_c, E_p, \sigma_{y1}, \sigma_{y2}, \alpha, adh, imp) \quad (5)$$

The Poisson's ratios of the steel pipe and polymeric material are 0.3 and 0.5, respectively. adh stands for the adhesion properties between the layers, which is considered to be the perfect or no adhesion condition in this study. Besides, the initial imperfection does not affect on the buckle propagation pressure. Therefore, the nondimensionalized form of Eq. (5) can be written as follows:

$$\frac{P_p}{E_p} = f\left(\frac{t_1}{r_1}, \frac{t_2}{r_2}, \frac{r_2}{r_1}, \frac{E_c}{E_p}, \frac{\sigma_{y1}}{E_p}, \frac{\sigma_{y2}}{E_p}, \alpha, adh\right) \quad (6)$$

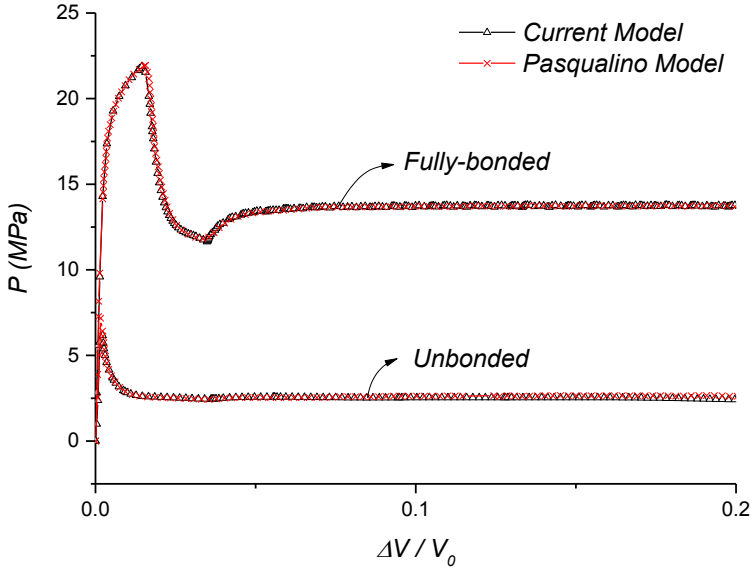

Figure 8: Pressure change in volume response of SP with G2 geometry

Table 3: Comparison of the buckle propagation pressure of SP

Model	Experiments[#] (MPa)	No adhesion[#] (MPa)	No adhesion (MPa)	Perfect adhesion[#] (MPa)	Perfect adhesion (MPa)	Max error %
SP.G1.P01	8.39	8.30	8.25	25.48	25.28	0.78
SP.G1.P02	7.89	8.03	8.10	24.87	25.13	1.04
SP.G2.P01	2.48	2.61	2.68	13.81	14.12	2.68
SP.G2.P02	2.28	2.62	2.57	14.33	13.92	1.91

[#]: Results from Lourenço *et al*. (2008).

Table 4 lists the value range for the selected parameters, and the internal surface radii of the inner and outer pipes are given in Table 1. The variation of the steel pipe's t/r ratio is from 0.03 to 0.09, which covers most of the thickness values specified for API 5L pipes. The steel grades consisting of X56, X65, X80, X100 and X120 for inner and outer pipes are considered. Moreover, the strain hardening parameter $\alpha(= E_p/E'_p)$ of the steel pipes is included, which can reflect the strain hardening effect of material in plastic deformation stage. Based on the Abaqus CAE package and the Python programming language, the series of models with different parameters shown in Table 4 are created and analyzed, respectively.

3.2 ADHESIVE PROPERTIES

The interactions between core and steel pipes in the tangential and normal directions are depending on the smoothness of the contact surfaces for steel pipes and interlayer adhesive strength, respectively, which have an impact on the propagation pressure capacity of SP. Figure 9 shows the pressure-volume response of SP during the propagation process. The propagation pressure of SP with the unbonded and fully bonded interface condition are 5.71 MPa and 45.79 MPa, respectively. It can be seen that the buckle propagation pressure of SP with fully-bonded condition is around 8 times the value of the one with unbonded condition.

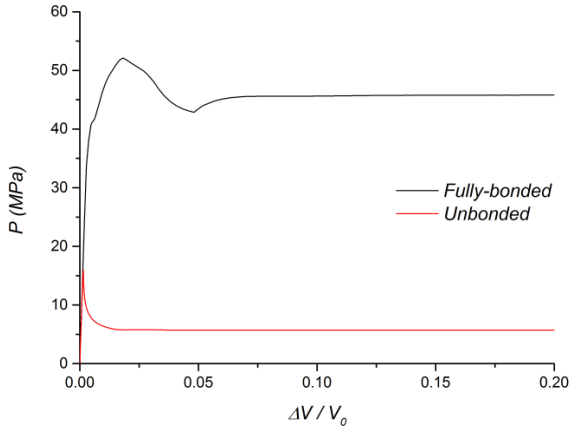

Figure 9: Pressure-volume response of SP with fully-bonded interface condition and unbonded condition during the propagation process.

3.3 GEOMETRIC CHARACTERISTICS

3.3(a) Thickness to Radius Ratio of Steel Pipes

Based on API 5L Specification for Line Pipe, the thickness to radius ratio varies from 0.03 to 0.09, which is applied for investigating the influence of thickness-to-radius ratio of steel pipes on the propagation pressure, viz., t_1/r_1 and t_2/r_2 varying from 0.03 to 0.09. Note that when varying the values of t_1/r_1, t_2/r is equal to 0.05, and vice versa.

The propagation pressure of SP with different thickness to radius ratio are shown in Figure 10. It can be seen that the buckle propagation pressure of SP increases with the thickness-to-radius ratio for both unbonded and fully bonded cases.

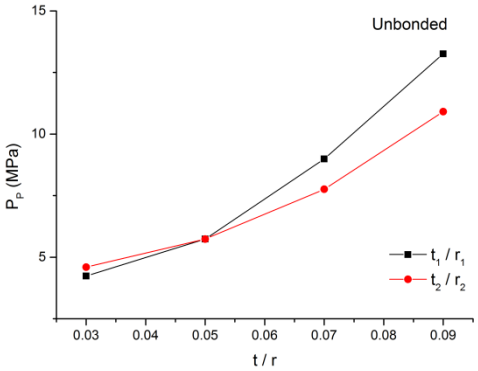

(a) SP with unbonded interface condition.

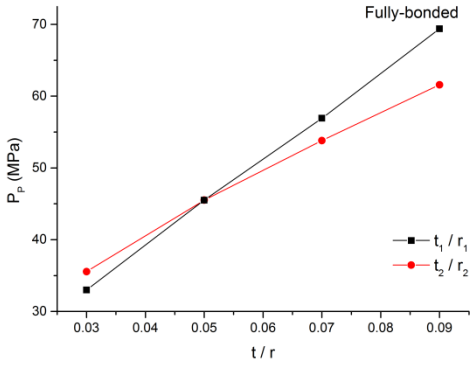

(b) SP with fully-bonded interface condition

Figure 10: Influence of the thickness-to-radius ratio on the buckle propagation pressure of SP

Table 4: Range of the parameters adopted in the parametric studies

t_1/r_1	t_2/r_2	r_1/r_2	E_c/E_p	σ_{y1}/E_p	σ_{y2}/E_p	α
0.03	0.03	0.489	0.1	0.001865 (X56)	0.001865 (X56)	25
0.05	0.05	0.580	0.01	0.002165 (X65)	0.002165 (X65)	50
0.07	0.07	0.636	0.001	0.002665 (X80)	0.002665 (X80)	100
0.09	0.09	0.727		0.003331 (X100)	0.003331 (X100)	1000
		0.818		0.003997 (X120)	0.003997 (X120)	10000

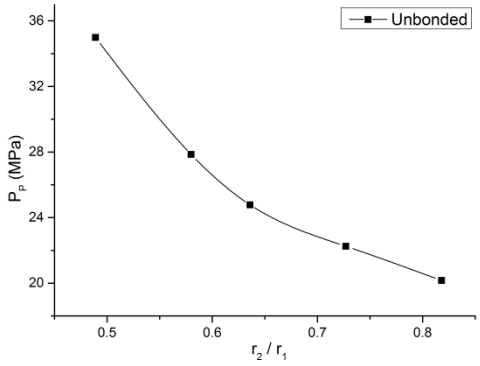

(a) SP with unbonded interface condition

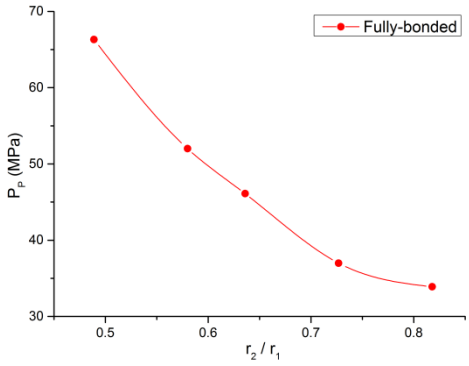

(b) SP with fully-bonded interface condition

Figure 11: Influence of the core thickness on the buckle propagation pressure of SP

Table 5: Geometries of the inner pipe

D_1 (in)	t_1 (in)	t_1/r_1	r_1/r_2
10.75	0.562	0.052	0.489
12.75	0.625	0.049	0.580
14	0.688	0.049	0.636
16	0.812	0.051	0.727
18	0.875	0.049	0.818

3.3 (b) Core thickness

In order to explore the core thickness on the propagation pressure of SP, different core thicknesses are selected by adjusting the diameter and thickness of inner pipe according to API 5L standard, as shown in Table 5. The diameter and thickness of the external pipe are 22 and 1.125 inch, respectively. Figure 11 shows the influence of the core thickness on the buckle propagation pressure of SP. The propagation pressure decreases with r_2/r_1 for both unbonded and fully bonded cases, which means that it increases with the core thickness.

3.4 STEEL GRADE

The steel grades of inner and outer pipes from X56 to X120 are considered to examine the effect of steel grade on the propagation pressure of SP. The simulated results of buckle propagation pressure with different steel grades are shown in Figure 12, where σ_{y1} and σ_{y2} are yielding stresses of inner and outer pipes, respectively. It can be seen that for a given geometry SP, the buckle propagation pressure with the unbonded or fully-bonded interface condition increases with the steel grades of inner and outer pipes. It is clearly observed that for a given geometry SP, the pressure of buckling propagation increases with the level of steel grade. However, In Figure 12(b), the margin between the curve of X120 and X100 is smaller comparing to the other margins. The main reason is that the failure mode for the SP with the inner steel pipe of X120 grade is the three-layer overall buckling, while the failure mode for the other SPs is the inner layer buckling. The same mechanism can be applied to explain the larger margin between the curve of X56 and X65 comparing to the other margins in Figure 12(d). The failure mode for the SP with the outer steel pipe of X56 grade is the inner layer buckling, while the failure mode for the other SPs is the three-layer overall buckling.

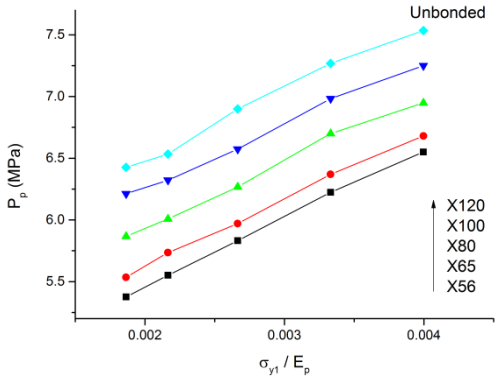

(a) SP with unbonded interface condition

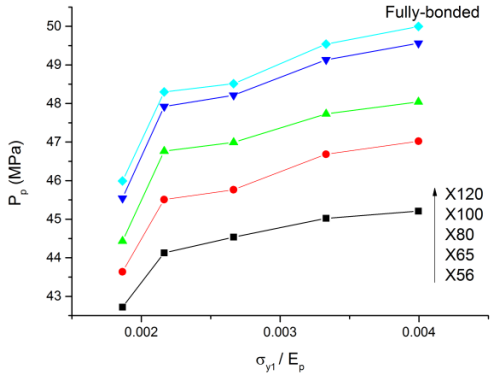

(b) SP with fully-bonded interface condition

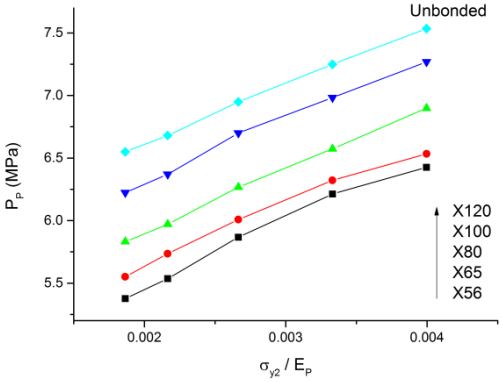

(c) SP with unbonded interface condition

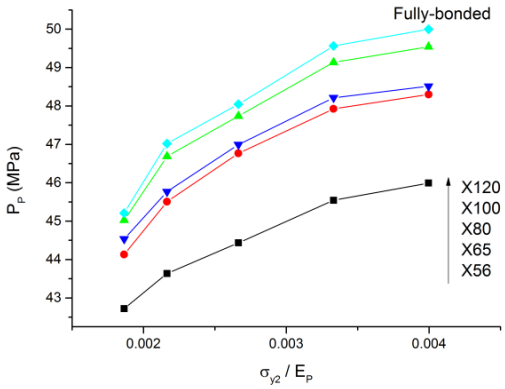

(d) SP with fully-bonded interface condition

Figure 12: Influence of the steel grade on the buckle propagation pressure of SP

4. CONCLUSIONS

This paper presents the buckle propagating behavior of sandwich pipes under external pressure in the quasi-static steady-state conditions. A three-dimensional finite element model for sandwich pipes is developed to analyze the buckle propagation phenomenon. 96 sandwich pipes are parametrically built to study the influence of material properties, geometric characteristics and adhesive properties on the propagation pressure. The following conclusions can be drawn:

- The adhesive properties between the layers have significant effects on the buckle propagation pressure. For the given case, it can be seen that the buckle propagation pressure of SP with fully-bonded condition is around 8 times the value of the one with unbonded condition.
- Increasing the t/r ratio and steel grades of inner and outer pipes can improve the propagation pressure of the system. Besides, the greater steel grade can drive the failure mode shift of SP from the inter layer buckling to three-layer overall buckling.

5. ACKNOWLEDGEMENTS

The work is supported by National Key Research and Development Plan (Grant No. 2016YFC0303704), National Natural Science Foundation of China (Grant No. 51879271 and No. 51509258).

6. REFERENCES

1. AN, C., *et al*. (2012) *Ultimate strength behaviour of sandwich pipes filled with steel fiber reinforced concrete*. OCEAN ENG, 55, 125-135.
2. AN, C., *et al*. (2014) *Collapse of sandwich pipes with PVA fiber reinforced cementitious composites core under external pressure*. OCEAN ENG, 82, 1-13.
3. ALBERMANI, F., *et al*. (2011) *Propagation buckling in deep sub-sea pipelines.* ENG STRUCT, 33(9), 2547-2553.
4. ARJOMANDI, K. and TAHERI, F. (2010) *Elastic buckling capacity of bonded and unbonded sandwich pipes under external hydrostatic pressure*. J MECH MATER STRUCT, 5(3), 391-409.
5. DYAU, JY. and KYRIAKIDES, S. (1993) *On the propagation pressure of long cylindrical shells under external pressure*. INT J MECH SCI, 35(8), 675-713.
6. ESTEFEN, SF., *et al*. (2005) *Strength analyses of sandwich pipes for ultra deepwaters*. J APPL MECH-T ASME, 72(4), 599–608.
7. GONG, SF., *et al*. (2012) *Buckle propagation of offshore pipelines under external pressure.* MAR STRUCT, 29(1), 115-130.
8. GONG, SF., *et al*. (2013) *Asymmetric collapse of offshore pipeline under external pressure.* SHIPS OFFSHORE STRUC, 8(2), 176–188.
9. FU, GM., *et al*. (2014) *Sandwich pipes with strain hardening cementitious composites (SHCC): Numerical analyses.* In: Proceedings of the 33rd International Conference on Ocean, Offshore and Arctic Engineering, San Francisco, USA. OMAE2014-23507.
10. HE, T., *et al*. (2015) *On the external pressure capacity of sandwich pipes with inter-layer adhesion layers.* APPL OCEAN RES, 52, 115-124.
11. KYRIAKIDES, S. and BOBCOCK, CD. (1981) *Experimental determination of the propagation pressure of circular pipes.* J PRESS VESS-T ASME, 103(4), 328-336.
12. KYRIAKIDES, S. (2002) *Buckle propagation in pipe-in-pipe systems.: Part I. Experiments*. INT J SOLIDS STRUCT, 39(2), 351-366.
13. KYRIAKIDES, S. and VOGLER, TJ. (2002) *Buckle propagation in pipe-in-pipe systems.*: *Part II. Analysis*. INT J SOLIDS STRUCT, 39(2), 367-392.
14. KYRIAKIDES, S. and NETTO, TA. (2004) *On the dynamic propagation and arrest of buckles in pipe-in-pipe systems.* INT J SOLIDS STRUCT, 41(20), 5463-5482.
15. KYRIAKIDES, S. and CORONA, E. (2006) *Mechanics of Offshore Pipelines Volume 1: Buckling and Collapse.* Elsevier, Oxford, UK.
16. KHALILPASHA, H. and ALBERMANI, F. (2014) *Textured deep subsea pipelines.* ENG STRUCT, 68, 224-235.
17. LOURENÇO, M., *et al*. (2008) *Core Material Performance on the Propagation Pressure of Sandwich Pipes.* In: Proceedings of the 27th International Conference on Ocean, Offshore and Arctic Engineering, Estoril, Portugal. OMAE2008-57507.
18. PALMER, AC. and MARTIN, JH. (1975) *Buckle propagation in submarine pipeline.* NATURE, 254, 46-48.
19. SHOWKATI, H. and SHAHANDEH, R. (2010) *Experiments on the buckling behavior of ring-stiffened pipeline under hydrostatic pressure.* J ENG MECH, 136 (4), 464-471.
20. CASTELLO, X. and ESTEFEN, SF. (2007) *Limit strength and reeling effects of sandwich pipes with bonded layers.* INT J MECH SCI, 49(5), 577-588.
21. XU, QB., *et al*. (2016) *Collapse analyses of sandwich pipes under external pressure considering inter-layer adhesion behavior.* MAR STRUCT, 50, 72-94.

